AN EFFICIENT DAMPING TECHNIQUE FOR THE UNSTABLE HYSTERETIC ROTOR WHIRL BY PROPER SUSPENSION SYSTEMS

Francesco Sorge[1], Marco Cammalleri [2]

[1]Department of Mechanics, University of Palermo, Italy
+39 091 6657157, E-mail: sorge@dima.unipa.it
[2]Department of Mechanics, University of Palermo, Italy
+39 091 6657160, E-mail: cammalleri@dima.unipa.it

ABSTRACT

This paper shows how the destabilising influence of the shaft hysteresis on the supercritical rotor whirl can be efficiently counterbalanced by external dissipative sources. After calculating the steady whirling paths of the rotor and the bearing due to unbalance, the stability is checked by the Routh-Hurwitz procedure, investigating the influence of the stiffness anisotropy of the supports. A fairly interesting result is that the instability phenomena can be conveniently prevented by different suspension stiffness in the horizontal and vertical planes.

Keywords: conical whirl, hysteresis, rotating machinery

INTRODUCTION, NATURAL MODES AND STEADY MOTION

The supercritical instability trend of rotor whirl motions because of the shaft hysteresis is generally rather modest but may become important in some applications, e. g. in long carbon/epoxy driveshafts with relevant hysteretic resistances [1]. Nevertheless, the hysteretic instability can be efficiently counterbalanced by other dissipative sources. Recent researches [2,3] show that elastic journal box suspensions with dry friction damping yield an excellent contrast to the critical flexural speeds, and exert also a strong quenching action on the unstable hysteresis motions.

The stabilizing properties of the external viscous damping are generally detected in the literature for centred rotor-support arrangements (e. g. see [4]). The present analysis considers a non-centred assembly, with different suspension stiffness in the horizontal and vertical planes. The stability is checked by the classical Routh-Hurwitz procedure, investigating the influence of several mechanical characteristics and finding that the hysteretic phenomena can be conveniently prevented by planning different suspension stiffness in the horizontal and vertical planes.

Figure 1 shows a rotor-suspension system and may be used as a reference for the notation. The approach is similar to [3]. The rotor is affected by the unbalance e and the assembly is horizontal in the gravitational field $\boldsymbol{g}$. The frame $C\xi\eta\zeta$ does not partake in the main rotating motion, but performs only the small elastic rotations φ and ψ around the axes x and y. The differentiation with respect to the angular time variable $\theta = \omega t$ is indicated with primes, whence $d(\ldots)/dt = \omega(\ldots)'$, etc. Introducing a reference shaft stiffness k (e. g. $k = 48EI/l^3$ for self-aligning bearings) and a reference critical speed $\omega_c = \sqrt{k/m}$, the angular speed ratio $\Omega = \omega/\omega_c$, the stiffness ratios, $K_{3x} = k_{3x}/k$, $K_{3y} = k_{3y}/k$, $K_{4x} = k_{4x}/k$, $K_{4y} = k_{4y}/k$ and the dimensionless gravity parameter $\Gamma = mg/ek$ are also introduced.

External viscous dissipation sources are supposed to act on the rotor translation and rotation and the coefficients c_t [N×s/m] and c_r [N×s×m] are introduced, together with the damping factors $d_1 = 0.5c_t\omega_c/k$ and $d_2 = 0.5c_r\omega_c/(kl^2)$. Likewise, the damping factors $d_{3x} = 0.5c_{3x}\omega_c/k$, $d_{3y} = 0.5c_{3y}\omega_c/k$, $d_{4x} = 0.5c_{4x}\omega_c/k$, $d_{4y} = 0.5c_{4y}\omega_c/k$, are ascribed to the horizontal and vertical motions of the supports. The shaft is considered mass-less, elastic and hysteretic, and the internal dissipative force is assumed proportional to the velocity $\mathbf{v}_{\text{rel.}}$ of point O_1 relative to a reference system $O_3\xi_0\eta_0\zeta_0$ having the coordinate axis ζ_0 through the shaft end section centres and rotating rigidly at the same angular speed ω (see detail of Fig. 1). Indicating the dimensionless distances of the rotor from the shaft ends with $L_3 = -z_3/l$ and $L_4 = z_4/l$, where l is the shaft length, the components of $\mathbf{v}_{\text{rel.}}$ in the fixed frame are $v_{\text{rel.},x} = \dot{x}_1 - \dot{x}_3L_4 - \dot{x}_4L_3 + \omega(y_1 - y_3L_4 - y_4L_3)$ and $v_{\text{rel.},y} = \dot{y}_1 - \dot{y}_3L_4 - \dot{y}_4L_3 - \omega(x_1 - x_3L_4 - x_4L_3)$. The hysteresis force on the rotor is $\mathbf{F}_h = -c_h\mathbf{v}_{\text{rel.}}$, where c_h is a hysteretic coefficient, and the forces on the two supports are $\mathbf{F}_{3h} = -L_4\mathbf{F}_h$, $\mathbf{F}_{4h} = -L_3\mathbf{F}_h$.

In case of full rotor balancing, the equilibrium deflection plane of the shaft counter-rotates with speed $-\omega$ with respect to the frame $O_3\xi_0\eta_0\zeta_0$, the hysteretic work done during one single revolution is $L_h = c_h\oint\left(v^2_{\text{rel.},x} + v^2_{\text{rel.},y}\right)dt = c_h\omega\oint[(y_{1\text{eq.}} - y_{3\text{eq.}}L_4 - y_{4\text{eq.}}L_3)^2 + (x_{1\text{eq.}} - x_{3\text{eq.}}L_4 - x_{4\text{eq.}}L_3)^2]d\theta$ and, assuming this work proportional to the path area regardless of ω, the product $c_h\omega$ may be assumed constant. The presence of some unbalance induces a further rotating bending of the shaft with speed ω around the equilibrium configuration and, while for

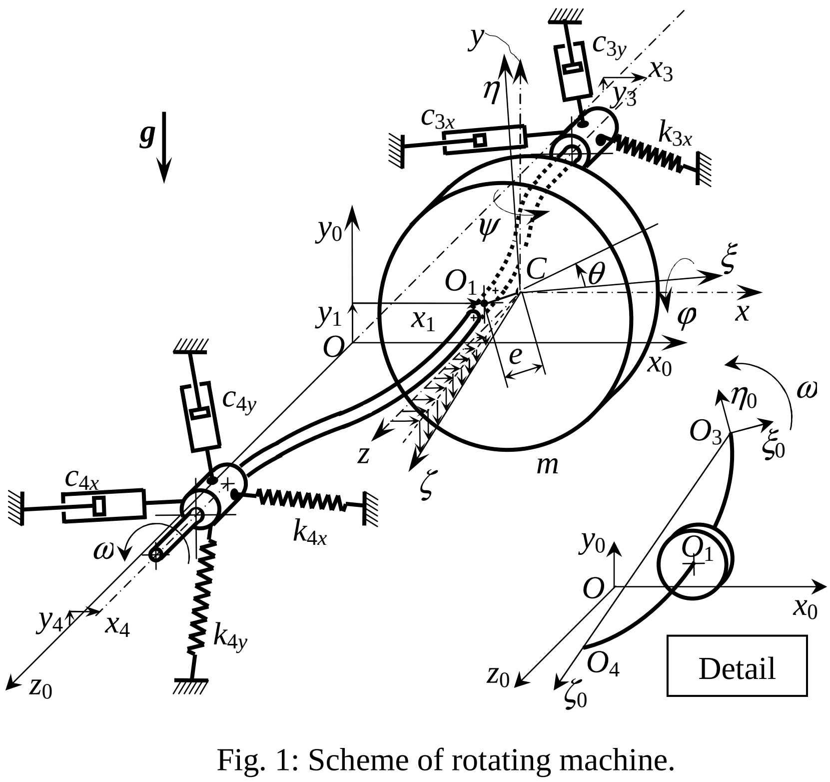

Fig. 1: Scheme of rotating machine.
Detail: reference system rotating with end sections

symmetric support stiffness this motion is rigid with the frame $O_3\xi_0\eta_0\zeta_0$ and uninfluential on the overall dissipation, in case of anisotropic stiffness ($K_{3x} \neq K_{3y}$, $K_{4x} \neq K_{4y}$), the unbalanced trajectories are elliptical and take double looped shapes in the rotating reference $O_3\xi_0\eta_0\zeta_0$, where, however, they are covered by twice the shaft frequency (2ω). According to [5], the two dissipative cycles can be dealt with separately and two different hysteresis coefficients c_h can be defined, the one, c_{h1}, for the frequency ω and the other, c_{h2}, for the double frequency 2ω. As it is reasonable to assume $\omega c_{h1} = 2\omega c_{h2} = h$ [5], where h is a hysteresis constant of the material, two hysteresis factors can be introduced, $d_{h1} = 0.5h/k$ for the relative rotation of the equilibrium deflection plane, and $d_{h2} = 0.25h/k = d_{h1}/2$ for the elliptical motion due to unbalance.
Scaling all displacements by the rotor eccentricity e and all rotations by e/l as in [3], the dimensionless displacement-rotation vectors $\mathbf{X} = \{X_1, X_2, X_3, X_4\}^T$ and $\mathbf{Y} = \{Y_1, Y_2, Y_3, Y_4\}^T$ may be introduced, where, using the subscripts 1, 3, 4 as in Fig. 1 for the rotor and support displacements and 2 for the rotor tilt around y or x, it was put $X_j = x_j/e$, $Y_j = y_j/e$, for $j \neq 2$, $X_j = \psi l/e$, $Y_j = -\varphi l/e$, for $j = 2$. Scaling all forces and moments by ke and kel respectively, calculating by the usual way the dimensionless stiffness matrices $\mathbf{K}_{jz}$ for $j = x$ or y (inflexion planes xz and yz), defining the dimensionless hysteretic matrices $\mathbf{H}_i$ for $i = 1$ or 2 (frequency ω and 2ω),

$$\mathbf{H}_i = d_{hi}\begin{bmatrix} 1 & 0 & -L_4 & -L_3 \\ 0 & 0 & 0 & 0 \\ -L_4 & 0 & L_4^2 & L_3L_4 \\ -L_3 & 0 & L_3L_4 & L_3^2 \end{bmatrix} \tag{1}$$

introducing the dimensionless diametral and axial moment of inertia of the rotor, $J_d = j_d/ml^2$ and $J_a = j_a/ml^2$, where j_d and j_a are the true moments, the equations of motion can be written in the form

$$\begin{aligned} &\mathbf{K}_{xz}\mathbf{X} + 2\Omega\mathbf{D}_{xz}\mathbf{X}' + 2\mathbf{H}_i(\mathbf{X}' + \mathbf{Y}) + \Omega^2\mathbf{M}\mathbf{X}'' + \Omega^2\mathbf{G}\mathbf{Y}' = \{\Omega^2\cos\theta \quad 0 \quad 0 \quad 0\}^T \\ &\mathbf{K}_{yz}\mathbf{Y} + 2\Omega\mathbf{D}_{yz}\mathbf{Y}' + 2\mathbf{H}_i(\mathbf{Y}' - \mathbf{X}) + \Omega^2\mathbf{M}\mathbf{Y}'' - \Omega^2\mathbf{G}\mathbf{X}' = \{\Omega^2\sin\theta - \Gamma \quad 0 \quad 0 \quad 0\}^T \end{aligned} \tag{2a,b}$$

where $\mathbf{D}_{jz}$ ($j = x, y$), $\mathbf{M}$ and $\mathbf{G}$ are diagonal and are the viscous, mass and gyroscopic matrices, whose coefficients are (d_1, d_2, d_{3j}, d_{4j}), (1, J_d, 0, 0) and (0, J_a, 0, 0) respectively.
The equilibrium configuration (constant solution) is easily obtained rewriting Eqs. 2 in the form $\mathbf{K}_{xz}\mathbf{X}_{\text{eq.}} + 2\mathbf{H}_1\mathbf{Y}_{\text{eq.}} = 0$, $\mathbf{K}_{yz}\mathbf{Y}_{\text{eq.}} - 2\mathbf{H}_1\mathbf{X}_{\text{eq.}} = -\Gamma\{1,0,0,0\}^T$, whence

$$\begin{aligned} &\mathbf{X}_{\text{eq.}} = \frac{32d_{h1}\Gamma L_3^2L_4^2}{1+\left(32d_{h1}L_3^2L_4^2\right)^2}\left[16L_3^2L_4^2 \quad 16L_3L_4(L_4-L_3) \quad 0 \quad 0\right]^T \\ &\mathbf{Y}_{\text{eq.}} = -\Gamma\left[\frac{16L_3^2L_4^2}{1+\left(32d_{h1}L_3^2L_4^2\right)^2} + \frac{L_3^2}{K_{4y}} + \frac{L_4^2}{K_{3y}} \quad \frac{16L_3L_4(L_4-L_3)}{1+\left(32d_{h1}L_3^2L_4^2\right)^2} - \frac{L_4}{K_{3y}} + \frac{L_3}{K_{4y}} \quad \frac{L_4}{K_{3y}} \quad \frac{L_3}{K_{4y}}\right]^T \end{aligned} \tag{3a,b}$$

As X_1 and X_2 are positive when $d_{h1} \neq 0$ and $L_4 > L_3$, the hysteresis produces a static bias of the inflexion plane concordant with the rotation.
The natural frequencies can be found cancelling the matrices $\mathbf{D}$ and $\mathbf{H}$ and the gravity-unbalance terms from Eqs. (2). Using the complex notation $\mathbf{X} = \mathbf{X}_0\exp(i\Omega_n\theta/\Omega)$, $\mathbf{Y} = -i\mathbf{Y}_0\exp(i\Omega_n\theta/\Omega)$, where $\Omega_n = \omega_n/\omega_c$, a fourth degree characteristic equation in Ω_n^2 can be obtained. Defining with $\mathbf{K}_{ij}^{kl}$ the 2×2 matrix extracted from the rows ij and columns kl of a

generic matrix **K** and putting $\overline{\mathbf{K}}_x = \mathbf{K}_{12}^{12} - \mathbf{K}_{12}^{34}\left(\mathbf{K}_{34xz}^{34}\right)^{-1}\mathbf{K}_{34}^{12}$, $\overline{\mathbf{K}}_y = \mathbf{K}_{12}^{12} - \mathbf{K}_{12}^{34}\left(\mathbf{K}_{34yz}^{34}\right)^{-1}\mathbf{K}_{34}^{12}$ for brevity ($\mathbf{K}_{xz}$ and $\mathbf{K}_{yz}$ differ only in the places 33 and 44), one gets

$$\left[\left(\overline{K}_{x11} - \Omega_n^2\right)\left(\overline{K}_{x22} - J_d\Omega_n^2\right) - \overline{K}_{x12}^2\right]\left[\left(\overline{K}_{y11} - \Omega_n^2\right)\left(\overline{K}_{y22} - J_d\Omega_n^2\right) - \overline{K}_{y12}^2\right] = \\ = \left(\overline{K}_{x11} - \Omega_n^2\right)\left(\overline{K}_{y11} - \Omega_n^2\right)J_a^2\Omega^2\Omega_n^2 \qquad (4)$$

The characteristic roots of Eq. (4) can be traced on Campbell diagrams $\Omega_n(\Omega)$,symmetric with respect to the origin. The choice between the plus or minus sign to be ascribed to $\Omega_n = \pm\sqrt{\Omega_n^2}$ has to be done, for each couple of amplitudes X_{j0} and Y_{j0}, so that their product $Y_{j0}\,X_{j0}$ is positive, whence the whirling motion is a progressive or retrograde precession for $\Omega_n > 0$ or $\Omega_n < 0$. It is remarkable that, for quite different stiffness of the supports, some whirling motions (e. g. of the rotor and of one support) may be counter-directed with respect to each other. All diagrams show the inclined asymptote J_a/J_d and the five horizontal asymptotes: $\Omega_n = 0$, $\Omega_n = \pm\sqrt{\overline{K}_{x11}}$, $\Omega_n = \pm\sqrt{\overline{K}_{y11}}$. The critical angular speeds, $\Omega_n = \pm\,\Omega$ (progressive or retrograde), are identified by the intersection of the locus with the bisectors of the axes. We may have seven or six critical speeds at most for $J_a/J_d < 1$ or $J_a/J_d > 1$ respectively (oblong or oblate ellipsoid of inertia of the rotor).
The forced whirling motions due to unbalance can be detected replacing $\mathbf{X} = \mathbf{X}_{c0}\cos\theta + \mathbf{X}_{s0}\sin\theta$, $\mathbf{Y} = \mathbf{Y}_{c0}\cos\theta + \mathbf{Y}_{s0}\sin\theta$ into Eqs. (2) and equating all terms in $\cos\theta$ and in $\sin\theta$ separately. A 16×16 algebraic system is obtainable, whose solution gives the elliptical paths of the rotor and the supports and the elliptical conical locus of the rotor axis. The principal amplitudes and orientation are given by

$$d_{\substack{\max.\\ \min.}} = 2\sqrt{\left[Y_{c0j}^2 + Y_{s0j}^2 + X_{c0j}^2 + X_{s0j}^2 \pm \sqrt{\left(Y_{c0j}^2 + Y_{s0j}^2 - X_{c0j}^2 - X_{s0j}^2\right)^2 + 4\left(X_{c0j}Y_{c0j} + X_{s0j}Y_{s0j}\right)^2}\,\right]\Big/2}$$

$$\tan 2\phi_j = 2\left(X_{c0j}Y_{c0j} + X_{s0j}Y_{s0j}\right)\Big/\left(X_{c0j}^2 + X_{s0j}^2 - Y_{c0j}^2 - Y_{s0j}^2\right)$$

Figure 2a shows examples of these loci, while Fig. 2b shows the two looped path of point O_1 in the rotating frame $O_3\xi_0\eta_0\zeta_0$. Dots refer to $\theta = 0$.

STABILITY

The stability can be controlled by the approach of the small perturbation, here indicated with tildes, replacing $\mathbf{X} = \mathbf{X}_{\text{steady}} + \tilde{\mathbf{X}}$ and $\mathbf{Y} = \mathbf{Y}_{\text{steady}} + \tilde{\mathbf{Y}}$ into Eqs. (2ab) and cancelling the steady variables and the forcing terms. The hysteresis factor d_{h1} will be used if the gravity prevails over the unbalance ($\Gamma >> 1$), d_{h2} will be used vice versa ($\Gamma << 1$). Assuming solutions of the type $\tilde{\mathbf{X}} = \tilde{\mathbf{X}}_0\exp(\sigma\theta/\Omega)$, $\tilde{\mathbf{Y}} = \tilde{\mathbf{Y}}_0\exp(\sigma\theta/\Omega)$, where σ is a characteristic number, one gets the twelfth degree characteristic equation

$$\det\begin{bmatrix} \mathbf{K}_{xz} + 2\sigma\mathbf{D}_{xz} + 2\sigma\mathbf{H}_i/\Omega + \sigma^2\mathbf{M} & 2\mathbf{H}_i + \sigma\Omega\mathbf{G} \\ -2\mathbf{H}_i - \sigma\Omega\mathbf{G} & \mathbf{K}_{yz} + 2\sigma\mathbf{D}_{yz} + 2\sigma\mathbf{H}_i/\Omega + \sigma^2\mathbf{M} \end{bmatrix} = 0 \qquad (5)$$

which can be condensed in the form $E_c(\sigma) = b_0\sigma^{12} + b_1\sigma^{11} + \ldots + b_j\sigma^{12-j} + \ldots + b_{11}\sigma + b_{12} = 0$. The coefficient $b_0 = 16J_d^2[d_{3x}d_{4x} + d_{hi}(d_{3x}L_3^2 + d_{4x}L_4^2)/\Omega]\;[d_{3y}d_{4y} + d_{hi}(d_{3y}L_3^2 + d_{4y}L_4^2)/\Omega]$ is quickly calculable and, choosing six values σ_i (i = 1, 2, …, 6) arbitrarily, it is simple to evaluate the determinants $E_c(\sigma_i)$ and $E_c(-\sigma_i)$ numerically and then compose two uncoupled 6×6 algebraic systems for the other unknown coefficients b_j:

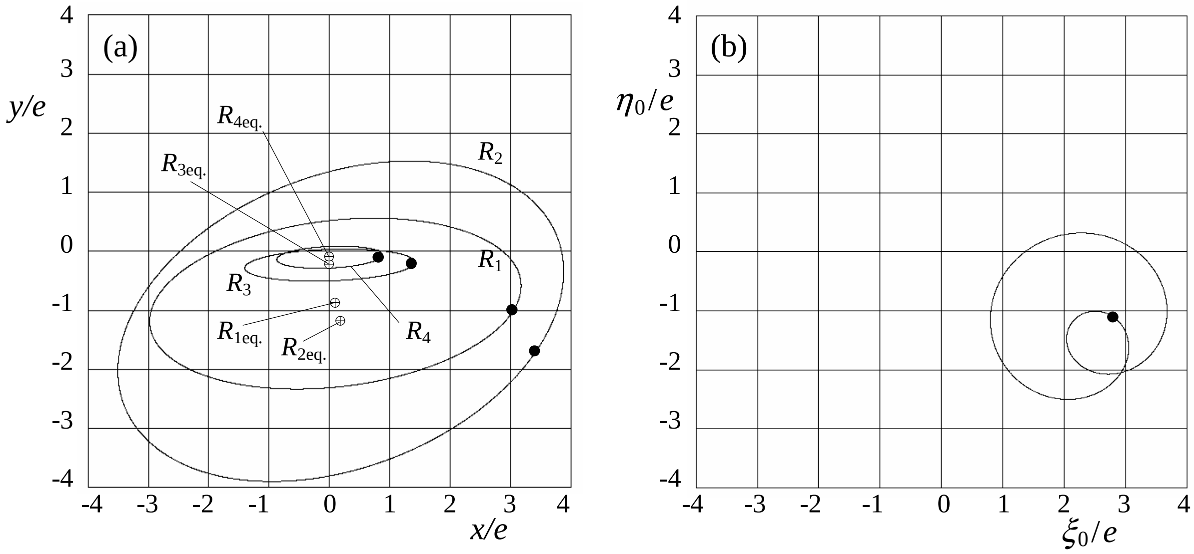

Fig. 2: (a) elliptical path of rotor centre ($R_1 = r_1/e$), of back and front journal box ($R_3 = r_3/e$ and $R_4 = r_4/e$) and of rotor axis ($R_2 = l\sqrt{\varphi^2+\psi^2}/e$), for $\Omega = 0.75$; (b) double looped path of point O_1 in the rotating frame $O_3\xi_0\eta_0\zeta_0$, for $\Omega = 0.8$.
Data $K_{3x} = K_{4x} = 1$, $K_{3y} = K_{4y} = 3$, $J_d = 0.1$, $J_a = 0.2$, $L_3 = 0.3$, $\Gamma = 1$, $d_1 = d_2 = d_{3x} = d_{4x} = d_{3y} = d_{4y} = 0.1$, $d_{h1} = 0.1$, $d_{h2} = 0.05$.

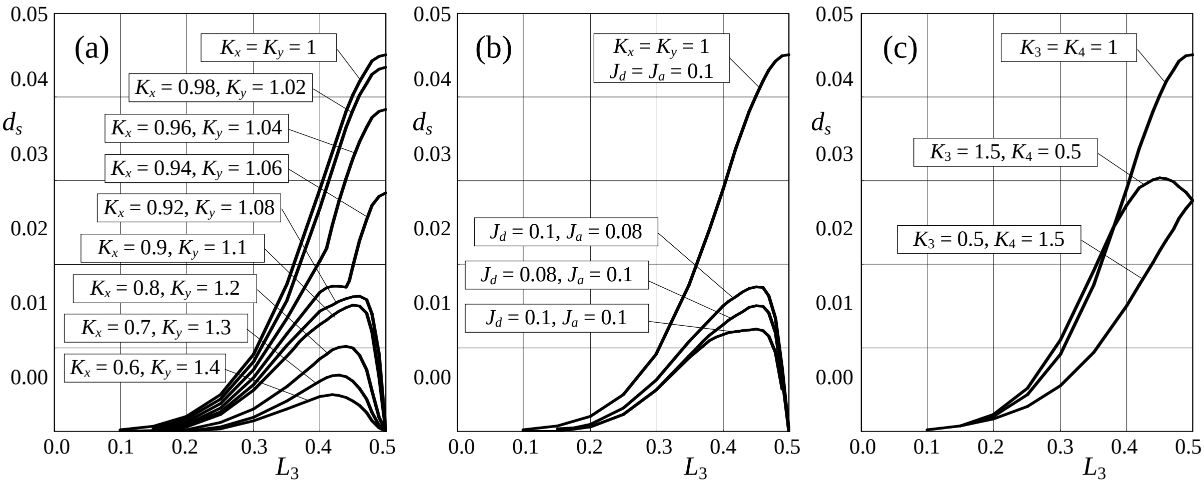

Fig. 3: Stability threshold for $d_s = d_{3x} = d_{4x} = d_{3y} = d_{4y}$ ($d_1 = d_2 = 0$, $d_{hi} = 0.02$)
(a): influence of support anisotropy ($J_d = 0.08$, $J_a = 0.1$); (b) gyro effect ($K_x = 0.9$, $K_y = 1.1$);
(c): influence of support asymmetry ($J_d = 0.1$, $J_a = 0.1$).

$$\begin{aligned}\frac{E_c(\sigma_i)+E_c(-\sigma_i)}{2} - b_0\sigma_i^{12} &= b_2\sigma_i^{10} + b_4\sigma_i^8 + b_6\sigma_i^6 + b_8\sigma_i^4 + b_{10}\sigma_i^2 + b_{12} \\ \frac{E_c(\sigma_i)-E_c(-\sigma_i)}{2} &= b_1\sigma_i^{11} + b_3\sigma_i^9 + b_5\sigma_i^7 + b_7\sigma_i^5 + b_9\sigma_i^3 + b_{11}\sigma_i\end{aligned} \quad \text{(for } i = 1 \text{ to } 6) \qquad (6)$$

Once calculated the b_j's, the stability analysis can be carried out looking for the sign changes in the sequence of the Routh-Hurwitz determinants. The application of this approach to the full speed range permits identifying the influence of the various physical parameters and finding the thresholds of stability, i. e. the viscous damping needed to nullify the destabilizing effect of hysteresis.
Figure 3a reports the stability threshold in dependence on the rotor location along the shaft and shows the influence of the support stiffness asymmetry in the horizontal and vertical

planes. The increase of the stiffness anisotropy improves the stability, specially if the rotor is centred in the shaft, in which case no external viscous dissipation is indeed required over a certain rather low asymmetry threshold. Figure 3b shows similar plots focusing on the gyro effect, which exerts a slight destabilizing effect: the case of a spherical ellipsoid of inertia ($J_a = J_d$) requires the lowest additional viscous damping to stabilize the rotor whirl. The influence of the elastic dissymmetry between the front and back suspension is shown in Fig. 3c, which might be prolonged for $L_3 > 0.5$ by mirror interchange of the two lower curves and indicates the convenience of a greater flexibility in the support closer to the rotor.

The stiffness anisotropy effect may be fairly highlighted considering a centred rotor with $K_{3x} = K_{4x} = K_x/2$, $K_{3y} = K_{4y} = K_y/2$, $d_1 = d_2 = 0$ and $d_{3x} = d_{4x} = d_{3y} = d_{4y} = d_s/2$, where the conical wobbling of the rotor axis is uncoupled with the other motions and is stable. Putting $X_1 = X$, $X_3 + X_4 = 2X_s$, $Y_1 = Y$, $Y_3 + Y_4 = 2Y_s$, $K_{jz11} = -2K_{jz13} = -2K_{jz14} = 1$, $2K_{jz33} = 2K_{jz44} = 1 + K_j$ (for $j = x$ or y), the stability approach leads to the sixth degree characteristic equation $(H^2 + 4d_{hi}^2)(A_x + \sigma^2)(A_y + \sigma^2) + \sigma^4 A_x A_y + \sigma^2 H[A_x(A_y + \sigma^2) + A_y(A_x + \sigma^2)] = 0$, where $H = 1 + 2d_{hi}\sigma/\Omega$, $A_x = K_x + 2d_s\sigma$, $A_y = K_y + 2d_s\sigma$. In the absence of hysteresis, this equation becomes $A_xA_y(1 + 1/\sigma^2)^2 + (A_x + A_y)(1 + 1/\sigma^2) + 1 = 0$, whence either $1 + 1/\sigma^2 = -1/A_x$ or $1 + 1/\sigma^2 = -1/A_y$, i. e. $2d_s\sigma^3 + (1 + K_{x\text{ or }y})\sigma^2 + 2d_s\sigma + K_{x\text{ or }y} = 0$, whose roots have negative real parts by the Routh-Hurwitz criterion. In the presence of hysteresis, it is verifiable that the fifth Routh-Hurwitz determinant RH_5 may become critical on increasing Ω. Assuming no viscous damping and supposing realistically that $(2d_{hi}/\Omega)^2 << 1$, this determinant may be approximated by $RH_5 \cong (2 + K_x + K_y)(K_xK_y)^2(2d_{hi}/\Omega)^3\{(K_y - K_x)^2 - 8d_{hi}^2[(K_y - K_x)^2 + 2(K_xK_y)^2\}$, whence the stability limit

$$\left|\frac{K_xK_y}{K_y - K_x}\right| < \sqrt{\frac{1}{16d_{hi}^2} - \frac{1}{2}} \tag{7}$$

is obtained for every angular speed. This result agrees with Figg. 3abc and points out the strong stabilizing effect of the elastic asymmetry of the supports.

Concluding, the anisotropic suspension stiffness of a rotating machine in the two transverse bending planes produces ellipticity of the rotor trajectory and of the axis conical locus, but appears indeed a very convenient technique to counteract the destabilising effect of the shaft internal hysteresis in the supercritical regime.

REFERENCES

[1] Montagnier, O., and Hochard, Ch., *Dynamic Instability of Supercritical Driveshafts Mounted on Dissipative Supports—Effects of Viscous and Hysteretic Internal Damping*, J. of Sound and Vibr., Vol. 305 (2007), 378–400.

[2] Sorge, F., *Rotor Whirl Damping by Dry Friction Suspension Systems*, ECOTRIB 2007, Europ. Conf. on Tribology, Ljubljana, Slovenija, 12-15/06/2007, published on MECCANICA, Springer, Vol. 43-6, 577-589.

[3] Sorge, F., *Damping of Rotor Conical Whirl by Asymmetric Dry Friction Suspension*, Journal of Sound and Vibration, v. 321 (1-2), 20/03/2009, 79-103.

[4] Gunter, E.J. jr., and Trumpler, P.R., *The Influence of Internal Friction on the Stability of High Speed Rotors with Anisotropic Supports*, ASME J. of Eng. for Industry, Vol. 116 (1969), 1105-1113.

[5] Wettergren, H.L., *On the Behavior of Material Damping Due to Multi-Frequency Excitation*, J. of Sound and Vibr., Vol. 206 (1997), 725-735.